Inorganic Chemistry
Article

Inorg. Chem. **2010**, *49*, 9823–9832 **9823**
DOI: 10.1021/ic100605t

Photoinduced Electron Transfer in Zn(II)porphyrin−Bridge−Pt(II)acetylide Complexes: Variation in Rate with Anchoring Group and Position of the Bridge

Erik Göransson,[†] Julien Boixel,[‡] Cyrille Monnereau,[‡] Errol Blart,[‡] Yann Pellegrin,[‡] Hans-Christian Becker,[†,§] Leif Hammarström,*[,†] and Fabrice Odobel*[,‡]

[†]*Department of Photochemistry and Molecular Science, Uppsala University, Box 523, SE-751 20 Uppsala, Sweden, and* [‡]*CEISAM, Chimie Et Interdisciplinarité, Synthèse, Analyse, Modélisation CNRS, UMR CNRS 6230, UFR des Sciences et des Techniques 2, rue de la Houssinière - BP 92208, 44322 NANTES Cedex 3, France.* [§]*Present address: Department of Chemical and Biological Engineering, Chalmers University of Technology, SE-412 96 Gothenburg, Sweden*

Received March 31, 2010

The synthesis and photophysical characterization of two sets of zinc porphyrin platinum acetylide complexes are reported. The two sets of molecules differ in the way the bridging phenyl−ethynyl unit is attached to the porphyrin ring. One set is attached *via* an ethynyl unit on the β position, while the other set is attached *via* a phenyl unit on the *meso* position of the porphyrin. These were compared with previously studied complexes where attachment was made *via* an ethynyl unit on the *meso* position. Femtosecond transient absorption measurements showed in all systems a rapid quenching of the porphyrin singlet state. Electron transfer is suggested as the quenching mechanism, followed by an even faster recombination to form both the porphyrin ground and triplet excited states. This is supported by the variation in quenching rate and porphyrin triplet yield with solvent polarity, and the observation of an intermediate state in the *meso*-phenyl linked systems. The different linking motifs between the dyads resulted in significant variations in electron transfer rates.

Introduction

Photoinduced electron transfer is a key process in the initial steps of photosynthesis.[1−3] Understanding of these reactions gives valuable information on how to develop and improve molecules and devices that can use solar energy to transform simple molecules into fuels[4,5] or to generate an electric current.[6−9] Studies of photoinduced electron transfer also give insight into charge-transport properties of molecules,[10−12] something which is of importance in the emerging field of molecular electronics.[13−16] Moreover, the signal-response behavior of photoinduced electron transfer may form a basis for opto-electronic molecular switches.[17−19]

In order to realize any of these functions, there is a need to find donor−acceptor systems that perform efficient charge separation upon illumination and have a charge-separated state that is energy-rich and long-lived enough to perform further work. Utilization of the inverted region effect, predicted by Marcus theory,[20,21] to give an activation barrier for recombination is a possible route to such a system. An alternative or complementary way of achieving a long-lived

*To whom correspondence should be addressed. E-mail: Leif.Hammarstrom@fotomol.uu.se (L.H.), Fabrice.Odobel@univ-nantes.fr (F.O.).

(1) Marcus, R. A.; Sutin, N. *Biochim. Biophys. Acta, Rev. Bioenerg* **1985**, *811*, 265–322.
(2) Wasielewski, M. R. *Chem. Rev.* **1992**, *92*, 435–461.
(3) *Oxygenic Photosynthesis: The Light Reactions*; Ort, D. R.; Yocum, C. F.; Heichel, I. F., Eds.; Kluwer Academic Publisher: Dordrecht, The Netherlands, 1996; Vol. *4*.
(4) Gust, D.; Moore, T. A.; Moore, A. L. *Acc. Chem. Res.* **2009**, *42*, 1890–1898.
(5) Magnuson, A.; Anderlund, M.; Johansson, O.; Lindblad, P.; Lomoth, R.; Polivka, T.; Ott, S.; Stensjö, K.; Styring, S.; Sundström, V.; Hammarström, L. *Acc. Chem. Res.* **2009**, *42*, 1899–1909.
(6) O'Regan, B.; Grätzel, M. *Nature* **1991**, *353*, 737–740.
(7) Hagfeldt, A.; Grätzel, M. *Acc. Chem. Res.* **2000**, *33*, 269–277.
(8) Islam, A.; Sugihara, H.; Hara, K.; Pratap Singh, L.; Katoh, R.; Yanagida, M.; Takahashi, Y.; Murata, S.; Arakawa, H. *New J. Chem.* **2000**, *24*, 343–345.
(9) Islam, A.; Sugihara, H.; Hara, K.; Singh, L. P.; Katoh, R.; Yanagida, M.; Takahashi, Y.; Murata, S.; Arakawa, H.; Fujihashi, G. *Inorg. Chem.* **2001**, *40*, 5371–5380.
(10) Davis, W. B.; Svec, W. A.; Ratner, M. A.; Wasielewski, M. R. *Nature* **1998**, *396*, 60–63.
(11) Davis, W. B.; Ratner, M. A.; Wasielewski, M. R. *Chem. Phys.* **2002**, *281*, 333–346.
(12) Albinsson, B.; Eng, M. P.; Pettersson, K.; Winters, M. U. *Phys. Chem. Chem. Phys.* **2007**, *9*, 5847–5864.
(13) Aviram, A.; Ratner, M. A. *Chem. Phys. Lett.* **1974**, *29*, 277–283.
(14) Tour, J. M. *Acc. Chem. Res.* **2000**, *33*, 791–804.
(15) Balzani, V. *Photochem. Photobiol. Sci.* **2003**, *2*, 459–476.
(16) Gust, D.; Moore, T. A.; Moore, A. L. *Chem. Commun.* **2006**, 1169–1178.
(17) Debreczeny, M. P.; Svec, W. A.; Wasielewski, M. R. *Science* **1996**, *274*, 584–587.
(18) Berberich, M.; Krause, A.-M.; Orlandi, M.; Scandola, F.; Würthner, F. *Angew. Chem., Int. Ed.* **2008**, *120*, 6718–6721.
(19) Wallin, S.; Monnereau, C.; Blart, E.; Gankou, J.-R.; Odobel, F.; Hammarström, L. *J. Phys. Chem. A* **2010**, *114*, 1709–1721.
(20) Marcus, R. A. *J. Chem. Phys.* **1965**, *43*, 679–701.
(21) Closs, G. L.; Miller, J. R. *Science* **1988**, *240*, 440–447.

Published on Web 10/04/2010

charge-separated state is to find linking motifs between the donor and acceptor that mediate electronic coupling better for the forward electron transfer (ET) than for the back electron transfer (BET). However, the electronic coupling element is difficult to predict *a priori*, with the result that much of the research in this area has focused on finding trends that can be used to design new molecular systems. In the present study, we investigate a series of donor−bridge−acceptor molecules where the bridge anchoring group and its position on the porphyrin donor are varied to affect the electronic coupling for forward electron transfer and recombination.

Porphyrins are versatile photosensitizers that have been used extensively to investigate and tune electron transfer in donor−acceptor systems.[2,12,22−28] Platinum(II)polypyridine complexes have also been used as the photoactive unit in molecular systems for photoinduced charge separation but less often used as ground state electron acceptors.[29−34] The use of a platinum complex as terminal electron acceptor is appealing, as some Pt complexes have been reported as reduction catalysts.[35−40] In an earlier study from our groups, we reported a series of six platinum terpyridine acetylide complexes linked to a metal porphyrin (Zn or Mg).[41] We found in all porphyrin−platinum dyads that the porphyrin excited state was rapidly quenched and returned to the ground state with time constants ranging from 2−20 ps. The quenching was attributed to electron transfer, followed by an even faster back reaction that prevented the buildup of a detectable signal. The rapid recombination was attributed to stronger electronic coupling for the back reaction. Since this prevented the buildup of a usable charge-transfer state, we wanted to systematically study modified porphyrin−platinum acetylide dyads with weaker electronic coupling and see whether the modifications have different effects on the primary photoinduced electron transfer and the subsequent recombination reaction.

In this work, we therefore present the synthesis and characterization of a series of electron donor−acceptor systems, each consisting of a zinc porphyrin unit (ZnP) as an electron donor linked *via* an oligo(*p*-phenylene-ethynylene) bridge (abbreviated OPE or ϕe) to a platinum terpyridine acetylide complex (Pt) as the electron acceptor (Chart 1). These dyads are closely related to those previously reported, but the way that the OPE bridge binds to the porphyrin ring has been altered with the aim of lowering the electronic coupling. Taking advantage of the platinum ion's ability to bind several acetylide ligands, the analogous triads (donor−acceptor−donor) with two porphyrin units linked to a single platinum ion were also synthesized and characterized. To allow for two acetylide groups binding to the platinum ion, an ester-substituted bipyridine was used as the ligand.

The first approach to modify the coupling was to attach the bridge to the porphyrin *via* a phenyl group instead of an ethynyl group, something which has been shown to have a pronounced effect on the electron transfer rates.[24,27] This is generally ascribed to steric interaction that forces the phenyl out of the porphyrin plane (see Figure 1a). The larger dihedral angle hinders the conjugated π system of the porphyrin from spreading out on the bridge, resulting in lower electronic coupling.[42,43] The second approach was to move the binding site of the bridge from the *meso* position to the β position. The two highest occupied orbitals (a_{1u} and a_{2u}) of the porphyrin are nearly degenerate, and both contribute almost equally to the electronic transitions seen in a UV−vis spectrum.[44] Furthermore, these two orbitals have distinctly different electron densities on the *meso* and β positions (Figure 1b), which could be used to affect the electronic coupling on these sites. Previous comparisons between *meso* and β positions have shown that the electronic coupling is lower at the β positions for both Dexter energy transfer[45] and photoinduced charge transfer.[28,46]

Experimental Section

General Methods. ^{1}H spectra were recorded on a Bruker 300 MHz or AMX 400 MHz Bruker spectrometer. Chemical shifts for ^{1}H NMR spectra are referenced relative to residual protium in the deuterated solvent ($CDCl_3$ δ = 7.26 ppm, d_6-DMSO δ = 2.54 ppm). Mass spectra were recorded on an EI-MS HP 5989A spectrometer or on a JMS-700 (JEOL LTD, Akishima, Tokyo, Japan) double focusing mass spectrometer of reversed geometry equipped with an electrospray ionization (ESI) source. Fast atom bombardment mass spectroscopy (FAB-MS) analyses were performed in an *m*-nitrobenzylalcohol matrix (MBA) on a ZAB-HF-FAB spectrometer. MALDI-TOF analyses were performed on a BIFLEX III Bruker Daltonics spectrometer in the positive linear mode at a 4 kV acceleration voltage.

Preparative thin-layer chromatography (preparative TLC) was performed with a Merck Kieselgel 60PF_{254}. Column chromatography was carried out with a Merk 5735 Kieselgel 60F

(22) Gust, D.; Moore, T. A.; Moore, A. L. *Acc. Chem. Res.* **1993**, *26*, 198–205.
(23) Nakano, A.; Osuka, A.; Yamazaki, T.; Nishimura, Y.; Akimoto, S.; Yamazaki, I.; Itaya, A.; Murakami, M.; Miyasaka, H. *Chem.—Eur. J.* **2001**, *7*, 3134–3151.
(24) Redmore, N. P.; Rubtsov, I. V.; Therien, M. J. *J. Am. Chem. Soc.* **2003**, *125*, 8769–8778.
(25) Imahori, H. *Org. Biomol. Chem.* **2004**, *2*, 1425–1433.
(26) Mataga, N.; Chosrowjan, H.; Taniguchi, S. *J. Photochem. Photobiol., C* **2005**, *6*, 37–79.
(27) Fortage, J.; Boixel, J.; Blart, E.; Hammarström, L.; Becker, H. C.; Odobel, F. *Chem.—Eur. J.* **2008**, *14*, 3467–3480.
(28) Song, H.-e.; Kirmaier, C.; Diers, J. R.; Lindsey, J. S.; Bocian, D. F.; Holten, D. *J. Phys. Chem. B* **2009**, *113*, 54–63.
(29) Harriman, A.; Hissler, M.; Trompette, O.; Ziessel, R. *J. Am. Chem. Soc.* **1999**, *121*, 2516–2525.
(30) Hissler, M.; McGarrah, J. E.; Connick, W. B.; Geiger, D. K.; Cummings, S. D.; Eisenberg, R. *Coord. Chem. Rev.* **2000**, *208*, 115–137.
(31) Chakraborty, S.; Wadas, T. J.; Hester, H.; Schmehl, R.; Eisenberg, R. *Inorg. Chem.* **2005**, *44*, 6865–6878.
(32) Bellows, D.; Goudreault, T.; Aly, S. M.; Fortin, D.; Gros, C. P.; Barbe, J.-M.; Harvey, P. D. *Organometallics* **2009**, *29*, 317–325.
(33) Liu, L.; Fortin, D.; Harvey, P. D. *Inorg. Chem.* **2009**, *48*, 5891–5900.
(34) Jiang, F.-L.; Fortin, D.; Harvey, P. D. *Inorg. Chem.* **2010**, *49*, 2614–2623.
(35) There is some uncertainty concerning the molecular integrity of Pt and Pd complexes under photocatalytic conditions, as pointed out in refs 39 and 40.
(36) Zhang, D.; Wu, L.-Z.; Li, Z.; Han, X.; Yang, Q.-Z.; Zhang, L.-P.; Tung, C.-H. *J. Am. Chem. Soc.* **2004**, *126*, 3440–3441.
(37) Ozawa, H.; Haga, M.-a.; Sakai, K. *J. Am. Chem. Soc.* **2006**, *128*, 4926–4927.
(38) Yamauchi, K.; Masaoka, S.; Sakai, K. *J. Am. Chem. Soc.* **2009**, *131*, 8404–8406.
(39) Du, P.; Schneider, J.; Fan, L.; Zhao, W.; Patel, U.; Castellano, F. N.; Eisenberg, R. *J. Am. Chem. Soc.* **2008**, *130*, 5056–5058.
(40) Lei, P.; Hedlund, M.; Lomoth, R.; Rensmo, H.; Johansson, O.; Hammarström, L. *J. Am. Chem. Soc.* **2008**, *130*, 26–27.
(41) Monnereau, C.; Gomez, J.; Blart, E.; Odobel, F.; Wallin, S.; Fallberg, A.; Hammarström, L. *Inorg. Chem.* **2005**, *44*, 4806–4817.
(42) Seth, J.; Palaniappan, V.; Wagner, R. W.; Johnson, T. E.; Lindsey, J. S.; Bocian, D. F. *J. Am. Chem. Soc.* **1996**, *118*, 11194–11207.
(43) Eng, M. P.; Albinsson, B. *Chem. Phys.* **2009**, *357*, 132–139.
(44) Gouterman, M. *J. Mol. Spectrosc.* **1961**, *6*, 138–163.
(45) Yang, S. I.; Seth, J.; Balasubramanian, T.; Kim, D.; Lindsey, J. S.; Holten, D.; Bocian, D. F. *J. Am. Chem. Soc.* **1999**, *121*, 4008–4018.
(46) Hayes, R. T.; Walsh, C. J.; Wasielewski, M. R. *J. Phys. Chem. A* **2004**, *108*, 2375–2381.

Chart 1. Outline of the Compounds Studied in This Work and Their Relation with the System Presented by Monnereau et al.[41a]

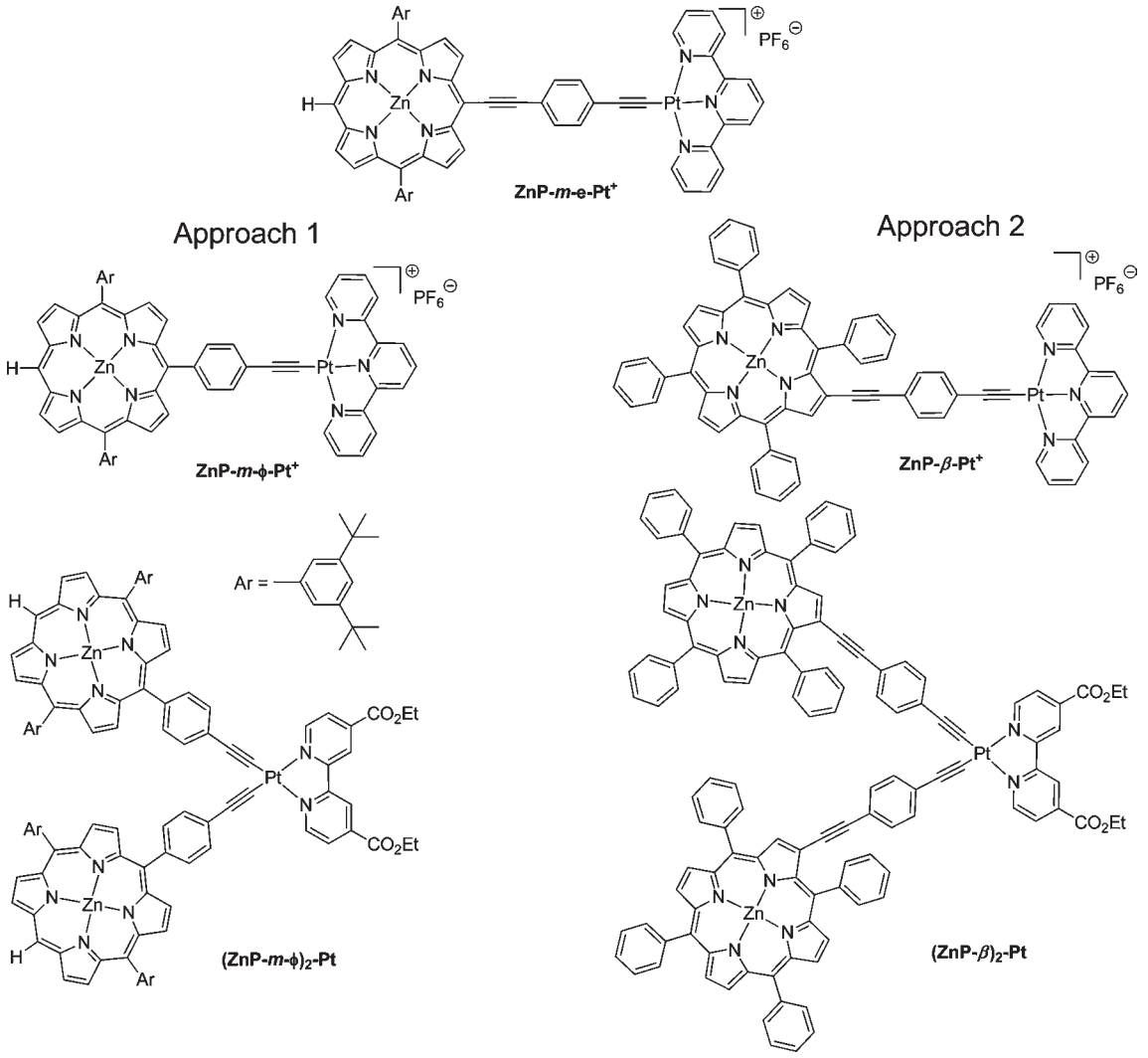

[a] Note on the abbreviations: The *meso* and β positions are denoted with "*m*" and "β", respectively, and the anchoring group to the porphyrin is denoted with "e" for ethynyl or "ϕ" for phenyl.

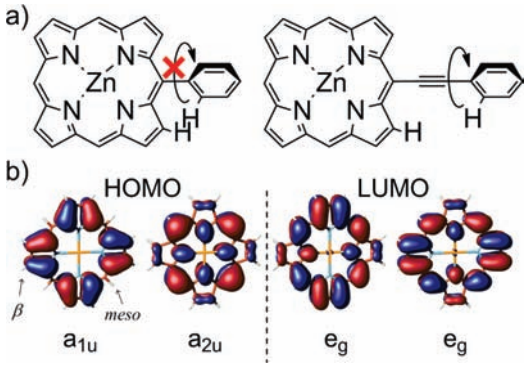

Figure 1. (a) Illustration of how steric interaction between the directly linked *meso* phenyl group and the hydrogen on the β position forces the phenyl out of the porphyrin plane. This does not occur when the phenyl is linked *via* an ethynyl group. (b) The two highest occupied orbitals and the two lowest unoccupied orbitals in a zinc porphyrin. Labels underneath indicate orbital symmetry.

(0.040−0.063 mm mesh). Air-sensitive reactions were carried out under argon in dry solvents and glassware. Chemicals were purchased from Aldrich and used as received. Spectroscopic grade N,N-dimethylformamide (DMF) and 2-methyl-tetrahydrofuran (2-MTHF) were purchased from Sigma-Aldrich (Sweden) and used as received. Compounds 4-(pinacolboron)-(triisopropylacetylene)benzene (**1**),[47] 3-bromo-5,10,15,20-tetraphenyl-porphyrin (**6**),[48] 10-bromo-5,15-di(3,5-diterbutylphenyl)-porphyrin (**2**),[63] 4-(tris(isopropyl)silylethynyl)-ethynyl benzene (**5**),[27] 5,15-bis-(3,5-ditertbutylphenyl)-10-phenyl-20-bromoporphyrin (**7**), chloroterpyridine platinum(II) (**9**),[49] and dichloro(4,4′-ethylcarboxylic ester-bipyridine)platinum(II) (**14**)[50] were prepared according to literature methods.

Absorption and Emission Spectroscopy. UV−vis absorption spectra were recorded on a Cary 50 absorption spectrometer, and steady-state emission spectra were measured on a Horiba SPEX Fluorolog 3 fluorometer. During emission measurements, the optical density was kept below 0.1 at the excitation wavelength. Low-temperature measurements were carried out in 2-MTHF glass at 77 K using a custom-made coldfinger setup.

(47) Godt, A.; Uensal, O.; Roos, M. *J. Org. Chem.* **2000**, *65*, 2837–2842.
(48) Vail, S. A.; Schuster, D. I.; Guldi, D. M.; Isosomppi, M.; Tkachenko, N.; Lemmetyinen, H.; Palkar, A.; Echegoyen, L.; Chen, X.; Zhang, J. Z. H. *J. Phys. Chem. B* **2006**, *110*, 14155–14166.
(49) Annibale, G.; Brandolisio, M.; Pitteri, B. *Polyhedron* **1995**, *14*, 451–3.
(50) McGarrah, J. E.; Eisenberg, R. *Inorg. Chem.* **2003**, *42*, 4355–4365.

Time-resolved fluorescence was measured with a time-correlated single photon counting setup (TCSPC), using either 570 or 405 nm excitation. The system has previously been described by Habenicht et al.[51] In summary, the 570 nm excitation was obtained from a Coherent OPA 9000 using the output from a Ti-sapphire laser (Coherent Reg A 900; 200 kHz, λ = 800 nm, fwhm 180 fs) as the laser source (IRF ~80 ps). For 405 nm excitation, a 405 nm LED at 5 MHz (fwhm 100 ps) was used (IRF ~100 ps). The emission was detected using a Hamamatsu MCP. A magic angle setup was ensured with two polarizers, and a scattered excitation light was blocked using a 640 nm bandpass filter.

Electrochemistry. Cyclic voltammetry was performed in a custom-made electrochemical cell using an Autolab potentiostat with a GPES electrochemical interface (Eco Chemie). Measurements were typically done in 200 μL of a 1 mM solution of the compounds in a deaerated (Ar (g)) DMF solution having 0.1 M $TBAPF_6$ as the supporting electrolyte. the working electrode was a 25 μm platinum microelectrode, and platinum wires were used as counter- and pseudo-reference electrodes. The pseudo-reference was calibrated for each sample by adding a small amount of decamethyl ferrocene ($FeCp^*_2$) as an internal standard ($FeCp^*_2{}^{+/0}$ = −0.125 vs SCE in DMF).[52]

Femtosecond-Transient Absorption. For a detailed description, see Andersson et al.[53] Briefly, the output from a Coherent Legend machine (1 kHz, λ = 800 nm, fwhm 80 fs) was split into a pump and a probe part. Using a TOPAS, the pump beam was transformed into the desired wavelength. Using a chopper, the pump frequency was reduced to 500 Hz, and with neutral density filters, the energy of each pulse at the sample was kept between 400 and 600 nJ. The pump pulse was transformed into a white-light continuum using a CaF_2 plate. The polarization of the pump was altered to ensure a magic angle with the probe, and the two beams were then focused and overlapped on a ~0.1 mm^2 area inside a 1 mm quartz cuvette. The samples had an OD of ~0.15 (Q-band excitation) or ~0.7 (Soret-band excitation) at the excitation wavelength, and the solution was stirred during measurement to minimize effects from photodegradation.

Data analysis was done in Igor Pro 5.[54] Kinetic data were globally fitted to the sum of exponentials with a Gaussian as a response function. Response function and time constants were linked between different wavelengths, while time zero and amplitudes were allowed to change. Difference spectra have been chirp compensated.

General Procedure for Coupling Reaction between Acetylene-Porphyrins and the Platinum Complex. The platinum complex **9** or **14** (typically 0.06 mmol) and the porphyrin **4** or **8** (with **9**, 1.2 equiv, 0.075 mmol; with **14**, 2.4 equiv, 0.150 mmol) were dissolved in distilled dichloromethane (35 mL). Diisopropylamine (0.7 mL) was added. The mixture was deaerated by N_2 bubbling with sonication, and a catalytic amount of copper iodide (≈1 mg) was added. The mixture was then stirred in the dark for 10 h, and water was added. The precipitate was isolated by filtration. A solid was recovered. See below for characterizations of the compounds. The proton labels used for the ^{1}H NMR data can be found in Supporting Information Chart S1.

ZnP-*m*-ϕ-Pt$^+$. Yield: 50%. ^{1}H NMR, δ (300 MHz, d_6-DMSO, 25 °C): 10.31 (s, 1H, H_{meso}); 9.48 (d, ^{3}J = 4.8 Hz, 2H, H_β); 9.41 (d, ^{3}J = 4.8 Hz, 2H, H_β); 8.92 (d, ^{3}J = 4.8 Hz, 2H, H_β); 8.89 (m, 3H, $2H_\beta$+$1H_{tpy}$); 8.55−8.74 (m, 8H, H_{tpy}); 8.17 (d, ^{3}J = 7.8 Hz, 2H, H_ϕ); 8.06 (m, 6H, $4H_{Ar}$+$2H_{tpy}$); 7.93 (d, ^{3}J = 7.8 Hz, 2H, H_ϕ); 7.85 (m, 2H, H_{Ar}); 1.55 (m, 36H, H_{tBu}). UV−vis (CH_2HCl_2), λ/nm ($\varepsilon/10^4$ M^{-1} cm^{-1}): 308 (2.3), 353 (1.5), 419 (73), 509 (0.4), 549 (3.3), 593 (0.6). HR-ESMS, calcd for $C_{71}H_{66}N_7{}^{64}Zn^{194}Pt$: 1274.4298. Found: 1274.4302 [M^+].

ZnP-β-Pt$^+$. Yield: 62%. ^{1}H NMR, δ (300 MHz, d_6-DMSO, 25 °C): 9.16 (m, 1H, H_{tpy}); 8.98 (s, 1H, H_β); 8.75 (d, ^{3}J = 3.0 Hz, 4H, H_β); 8.69 (d, ^{3}J = 4.6 Hz, 1H, H_β); 8.57 (d, ^{3}J = 4.6 Hz, 1H, H_β); 8.47−8.58 (m, 8H, H_{tpy}); 8.2 (m, 8H, H_{Ph}), 7.93 (m, 2H, H_{tpy}); 7.82 (m, 12H, H_{Ph}); 7.55 (d, ^{3}J = 8.1 Hz, 2H, H_ϕ); 7.35(d, ^{3}J = 8.1 Hz, 2H, H_ϕ). UV−vis (CH_2HCl_2), λ/nm ($\varepsilon/10^4$ M^{-1} cm^{-1}): 287 (3.4), 313 (3.2), 342 (2.3), 432 (19.3), 521 (0.83), 560 (1.8), 596 (0.91). HR-ESMS calcd for $C_{69}H_{42}N_7ZnPt$: 1226.2441. Found: 1226.2422 [M^+]. Elem Anal. calcd for C, 54.04; H, 3.52; N, 6.00. Found: C, 54.30; H, 3.37; N, 6.27.

(ZnP-*m*-ϕ)$_2$-Pt. ^{1}Yield: 45%. H NMR, δ (300 MHz, d_6-DMSO, 25 °C): 10.28 (s, 2H, H_{meso}); 10.05 (m, 2H, H_{bpy}); 9.47 (m, 4H, H_β); 9.1 (m, 2H, H_{bpy}), 8.91 (m, 12H, H_β); 8.48 (m, 2H, H_{bpy}); 8.16 (d, ^{3}J = 7.8 Hz, 4H, H_ϕ); 8.06 (s, 8H, H_{Ar}); 7.9 (d, ^{3}J = 7.8 Hz, 4H, H_ϕ); 7.8 (m, 4H, H_{Ar}), 4.51 (m, 4H, H_{CH2}); 1.54 (s, 72H, H_{tBu}); 1.23 (s, 6H, H_{CH3}). UV−vis (CH_2HCl_2), λ/nm ($\varepsilon/10^4$ M^{-1} cm^{-1}): 250 (2.8), 306 (2.9), 397 (3.6), 418 (33), 546 (1.7), 585 (0.35). HR-ESMS calcd for $C_{128}H_{126}N_{10}O_4Zn_2Pt$: 2193.8269. Found: 2193.8196 [M^+].

(ZnP-β)$_2$-Pt. Yield: 84%. ^{1}H NMR, δ (300 MHz, $CDCl_3$, 25 °C): 9.77 (d, ^{3}J = 5.1 Hz, 2H, H_{bpy}); 9.05 (s, 2H, H_{bpy}); 8.99 (s, 2H, H_β); 8.77 (s, 4H, H_β); 8.74 (s, 4H, H_β); 8.71 (d, ^{3}J = 4.8 Hz 2H, H_β); 8.60 (d, ^{3}J = 4.8 Hz, 2H, H_β); 8.39 (d, ^{3}J = 5.1 Hz, 2H, H_{bpy}); 8.2 (m, 16H, H_{Ph}); 7.75−7.84 (m, 24H, H_{Ph}); 7.45 (d, ^{3}J = 8.1 Hz, 4H, H_ϕ); 7.33 (d, ^{3}J = 8.1 Hz, 4H, H_ϕ); 4.48 (m, 4H, H_{CH2}); 1.23 (m, 6H, H_{CH3}). UV−vis (CH_2HCl_2), λ/nm ($\varepsilon/10^4$ M^{-1} cm^{-1}): 315 (7.5), 361 (3.4), 432 (44), 516 (1.6), 559 (4.4), 595 (2.1). MALDI-TOF calcd for $C_{124}H_{78}N_{10}O_4Zn_2Pt$: 2093.44. Found: 2093.69 [M^+].

Results

Synthesis of the Compounds. The preparation of the porphyrin−platinum complex systems requires the synthesis of the new zinc porphyrin units **4** and **8** substituted by a 1,4-bis(ethynyl)benzene linker (Scheme 1). Porphyrin **3** was synthesized by a Suzuki cross-coupling reaction between bromo-(*trans*-5,15-di-3−5-bis(*tert*-butyl))phenyl-zincporphyrin (**2**) and 4-(pinacolboron)-(tris(isopropyl)silylethynyl)benzene (**1**) with a 70% yield. On the other hand, β-substituted porphyrin **7** was obtained by a Sonogashira cross-coupling between β-bromo-tetraphenyl-porphyrin (**6**) and 4-(tris(isopropyl)silylethynyl)-ethynyl benzene (**5**) in 96% yield.[48,55] Porphyrins **4** and **8** were obtained from **3** and **7**, by removing the isopropylsilyl protecting group with tetrabutylammonium fluoride at room temperature in an almost quantitative yield.

The introduction of the platinum complex on the porphyrin sensitizer was achieved with a Sonogashira-type reaction either between the chloroterpyridine platinum(II)chloride (**9**) or dichloro(4,4′-ethylcarboxylic ester-bipyridine)platinum(II) (**14**) with porphyrin **4** or **8** in the presence of a base and a catalytic amount of copper iodide (Scheme 2).[41,56,57] The phenylacetylide platinum complexes **11** and **15** were also prepared as references using the same platinum precursors **9** and **14**, which were reacted with an excess of phenylacetylene (**10**).

(51) Habenicht, A.; Hjelm, J.; Mukhtar, E.; Bergström, F.; Johansson, L. B. Å. *Chem. Phys. Lett.* **2002**, *354*, 367–375.
(52) Aranzaes, J. R.; Daniel, M.-C.; Astruc, D. *Can. J. Chem.* **2006**, *84*, 288–299.
(53) Andersson, M.; Davidsson, J.; Hammarström, L.; Korppi-Tommola, J.; Peltola, T. *J. Phys. Chem. B* **1999**, *103*, 3258–3262.
(54) *Igor Pro 5*; WaveMetrics: Lake Oswego, OR.
(55) Lembo, A.; Tagliatesta, P.; Guldi, D. M.; Wielopolski, M.; Nuccetelli, M. *J. Phys. Chem. A* **2009**, *113*, 1779–1793.
(56) James, S. L.; Younus, M.; Raithby, P. R.; Lewis, J. *J. Organomet. Chem.* **1997**, *543*, 233–235.
(57) Whittle, C. E.; Weinstein, J. A.; George, M. W.; Schanze, K. S. *Inorg. Chem.* **2001**, *40*, 4053–4062.

Scheme 1. Synthesis of the Porphyrin Building Blocks **4** and **8**[a]

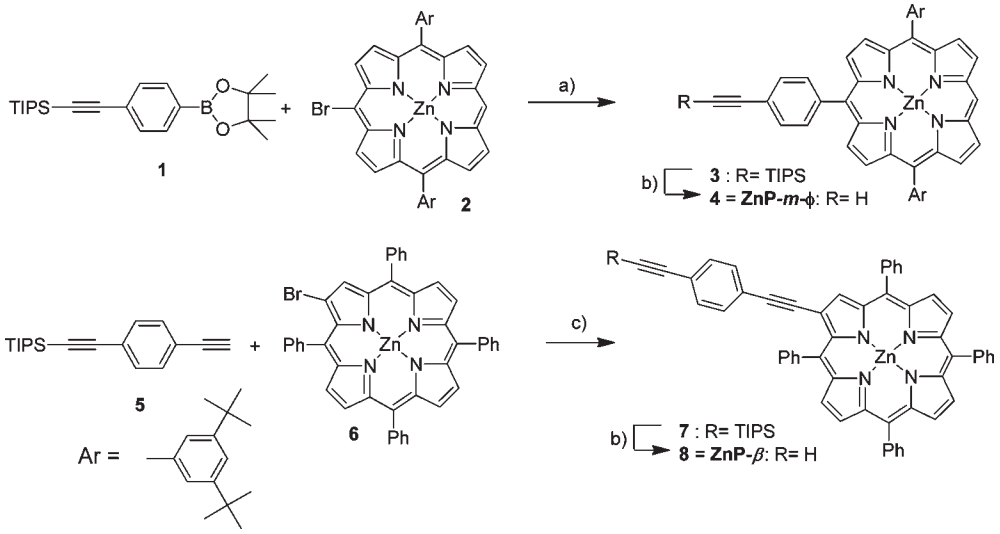

[a] Reagents and conditions: (a) PPh_3, $Ba(OH)_2$, 8 H_2O; Pd_2dba_3. $CHCl_3$, DME/H_2O (20%). (b) TBAF, THF (95%). (c) $AsPh_3$, $Pd(PPh_3)_4$, THF, Et_3N (96%).

Scheme 2. Synthesis of the Platinum Complex Zinc Porphyrin Conjugates[a]

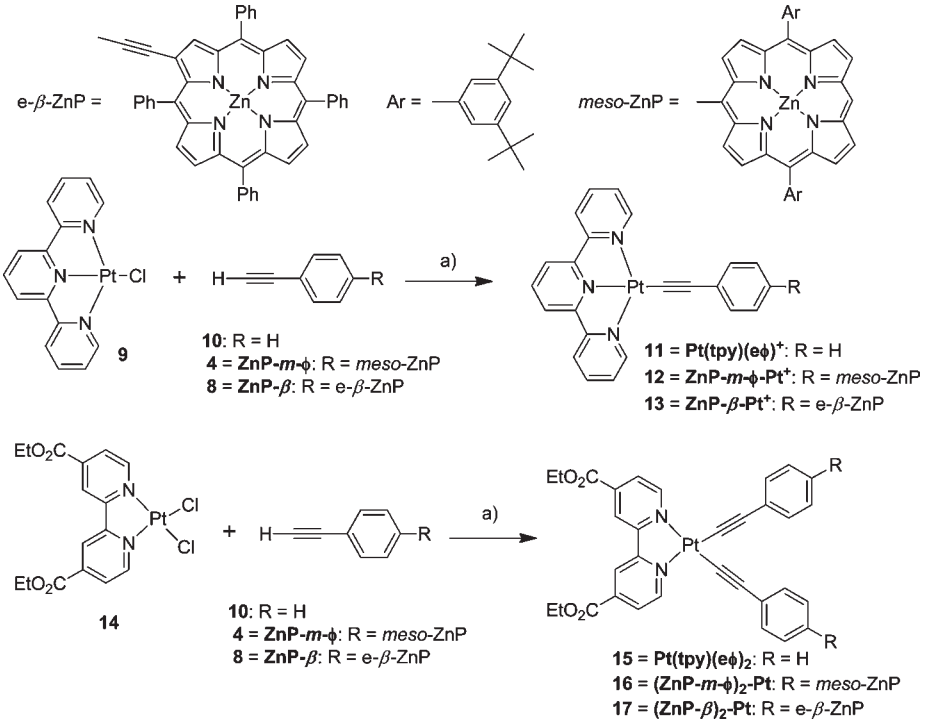

[a] Reagents and conditions: (a) CH_2Cl_2, iPr_2NH, CuI (**11**, 63%; **12**, 50%; **13**, 62%; **15**, 99%; **16**, 45%; **17**, 84%).

Electronic Absorption Spectra. Figure 2 shows the normalized absorption spectra of **ZnP-*m*-ϕ-Pt**$^+$, **ZnP-*m*-e-Pt**$^+$, and **ZnP-*β*-Pt**$^+$ in DMF. All three dyads feature spectra that are dominated by the porphyrin moiety. The MLCT band of the platinum unit is concealed by the porphyrin Soret band, but there are some features in the absorption spectrum that come from the acceptor unit. The *meso*-phenyl linked systems have the same sharp features as **ZnTTP** but are slightly blue-shifted. For the ethynyl substituted porphyrins, a distinct red shift and broadening of the spectral features compared to **ZnTTP** can be seen. This is attributed to a delocalization of the porphyrin π electrons onto the bridge, which in turn breaks the degeneracy of the *x* and *y* transitions in the Soret and Q bands.[58] The red shift of the spectrum caused by ethynyl linkage is larger for the *meso*-substituted porphyrins, while the broadening of the Soret band is more pronounced in the β-substituted systems.

A comparison of the spectral features of the new dyads with their respective building blocks can be found in Table 1 and in the Supporting Information (Figure S1).

(58) Lin, V. S.; DiMagno, S. G.; Therien, M. J. *Science* **1994**, *264*, 1105–1111.

Table 1. Absorption and Emission Properties of Studied Compounds in DMF

	λ_{abs}[a] (nm)	λ_{em} (RT)[a] (nm)	λ_{em} (77 K)[b] (nm)	E_{00} (eV)	relative Φ_{em}	τ_{em} (fraction) (ns)
Pt(bpy)(eϕ)$_2$	439	672	591	2.09[c]		
Pt(tpy)(eϕ)$^+$	314, 333, 347, 440	622	593	2.08[c]		
ZnTTP	306, 406, 426, 560, 600	608, 660		2.04[d]		1.9 (0.96)
ZnP-*m*-ϕ	310, 423, 555, 594	599, 650	770	2.07[d]	1[e]	2.4 (0.91)
ZnP-*β*	439, 569, 607	621, 673	810	2.01[d]	1[f]	1.6 (0.95)
ZnP-*m*-ϕ-Pt$^+$	349, 423, 554, 594	598, 649		2.07[d]	0.04[e]	< 0.04
(ZnP-*m*-ϕ)$_2$-Pt	310, 423, 554, 594	600, 651		2.07[d]	0.15[e]	< 0.04
ZnP-*β*-Pt$^+$	439, 569, 606	621, 674		2.01[d]	0.30[f]	0.05 (0.69)
(ZnP-*β*)$_2$-Pt	319, 439, 569, 605	621, 675		2.01[d]	0.07[f]	0.07 (0.88)
ZnP-*m*-e-Pt$^+$	445, 574, 626	632, 696		1.97[d]	0.16[g]	< 0.04[g]

[a] Peak position. [b] Measured in 2-MTHF glass at 77 K. Only phosphorescence peaks reported. [c] From 77 K emission peak. [d] From $[(\lambda_{abs})^{-1} + (\lambda_{emi,\ RT})^{-1})]/2$. [e] Relative emission quantum yield, using **ZnP-*m*-ϕ** as a reference. [f] Relative emission quantum yield, using **ZnP-*β*** as a reference. [g] From Monnereau et al.[41]

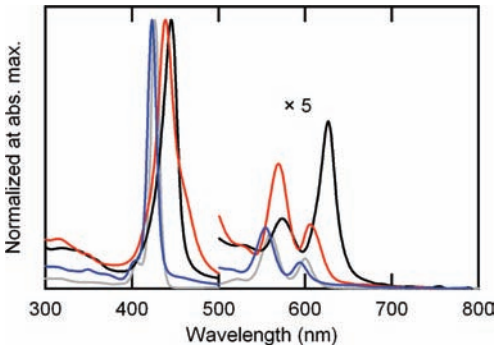

Figure 2. Normalized absorption spectra of **ZnP-*m*-φ-Pt$^+$** (blue), **ZnP-*β*-Pt$^+$** (red), **ZnP-*m*-e-Pt$^+$** (black), and **ZnTTP** (gray) in DMF. The Q-band region is magnified five times for clarity.

The coordination of the platinum moiety to the porphyrin causes almost no shifts of the spectral peaks, but it has some influence on the shape of the spectra. This is most clearly seen for the β-linked systems, which features an additional broadening of the porphyrin Soret band when the porphyrin is attached to the platinum acceptor (Figure S1b). In 2-MTHF, which is less polar than DMF, all the porphyrin peaks are slightly blue-shifted (SI: Figure S2 and Table S1), but the general shape of the spectrum is the same as in DMF.

Steady-State Emission. The emission spectra of the porphyrin references follow the trend from the absorption with the **ZnP-*m*-ϕ** emission slightly blue-shifted and **ZnP-*β*** red-shifted compared to **ZnTTP** (see Table 1 and Supporting Information Figure S3). The donor−acceptor complexes have emission spectra that are very similar to their respective porphyrin reference but with lower intensity (4−30% compared to the references). When changing solvent to 2-MTHF, the emission is shifted to shorter wavelengths by about 5 nm. The triplet states of **ZnP-*m*-ϕ** and **ZnP-*β*** were studied in 2-MTHF at 77 K. With gated detection, it was possible to separate the weak phosphorescence from the tail of the fluorescence, and peaks were found at 770 and 810 nm. The emission from the platinum polypyridyl complexes could not be detected in the dyads, but in DMF the platinum references featured a broad emission peak at 622 nm (**Pt(tpy)(eϕ)$^+$**) and 672 nm (**Pt(bpy)(eϕ)$_2$**), which is in agreement with previous studies.[41,50,57,59] In frozen glass (2-MTHF, 77 K), there is a substantial reduction in the Stokes shift, and the emission from both platinum references is found around 590 nm.

Time-Resolved Emission. Time-correlated single photon counting (TCSPC) measurements on the *meso*-phenyl-substituted dyads showed rapidly quenched emission. Deconvoluting the data with the instrument response function resulted in lifetimes < 40 ps, which is below the limit we can reliably resolve. The β-substituted dyads also featured a rapid component, which was fitted to 0.05 and 0.07 ns for **ZnP-*β*-Pt$^+$** and **(ZnP-*β*)$_2$-Pt**, respectively. Changing solvent to 2-MTHF resulted in longer lifetimes for **ZnP-*m*-ϕ-Pt$^+$** and **(ZnP-*m*-ϕ)$_2$-Pt**, but still below the time resolution limit. **ZnP-*β*-Pt$^+$** also featured a longer lifetime in 2-MTHF, while **(ZnP-*β*)$_2$-Pt** surprisingly had a shorter lifetime, which was < 40 ps. The time constants discussed above were the dominating components, but all samples also featured smaller fractions that had lifetimes similar to those of the references (2.4 ns for **ZnP-*m*-ϕ** and 1.6 ns for **ZnP-*β*** in DMF). These fractions of unquenched porphyrins are probably the cause of most of the emission observed in steady-state measurements (Table 1).

Electrochemistry. Cyclic voltammetry was performed in DMF to get an estimation of the driving force for electron transfer (Table 2). The first reduction and oxidation waves were both reversible in the dyads and the porphyrin references, while the platinum references featured a reversible reduction and an irreversible oxidation wave. The potentials of the reference molecules agree with those previously reported,[41,50,60] and these potentials were used to assign the half-wave potentials observed for the dyad systems.

Ultrafast Transient Absorption. *meso*-Phenyl Linked Dyads. Upon excitation of **ZnP-*m*-ϕ** at 595 nm, the lowest excited S_1 state of the zinc porphyrin is formed (Figure S4a, Supporting Information). The difference spectrum is dominated by a broad absorption covering the whole spectrum and with a peak at 450 nm. The excited state absorption is overlapped with the distinct bleach from the ground state absorption, and there is also an apparent bleach around 650 nm due to stimulated emission. The singlet spectrum evolves into the triplet spectrum (τ = 2.4 ns), which remains unchanged within the experimental time window. The triplet and singlet spectra are notoriously similar, but they can be differentiated because the triplet has a sharper peak at 450 nm and is lacking the bleach feature from stimulated emission at 650 nm.

(59) Yam, V. W.-W.; Tang, R. P.-L.; Wong, K. M.-C.; Cheung, K.-K. *Organometallics* **2001**, *20*, 4476–4482.

(60) Lembo, A.; Tagliatesta, P.; Guldi, D. M. *J. Phys. Chem. A* **2006**, *110*, 11424–11434.

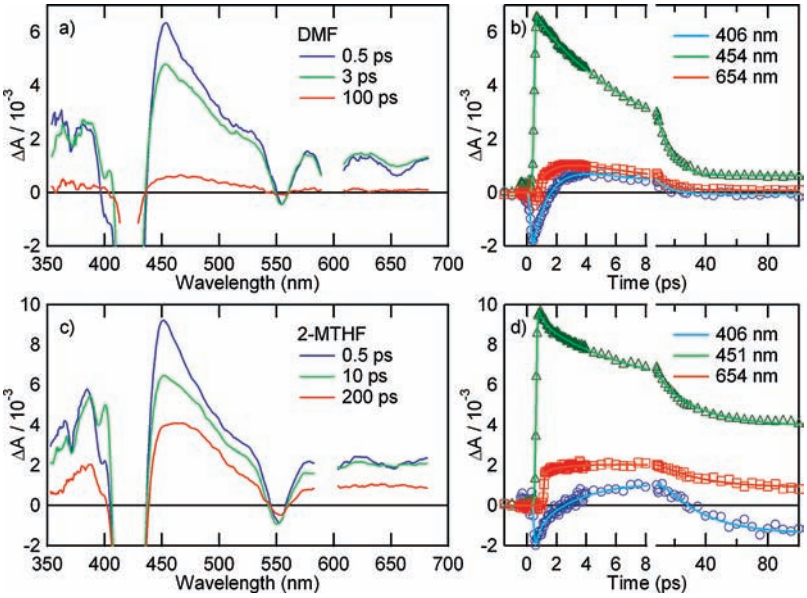

Figure 3. Results from pump−probe measurements on **ZnP-*m*-ϕ-Pt**$^+$ in DMF (a and b) and 2-MTHF (c and d) (λ_{exc} = 595 nm). (a) Difference in DMF, spectra at 0.5 ps (blue), 3 ps (green), and 100 ps (red). (b) Kinetic data in DMF (markers) and fit (full line) at 406 nm (circles, blue), 454 nm (triangles, green), and 654 nm (squares, red). (c) Difference in 2-MTHF, spectra at 0.5 ps (blue), 10 ps (green), and 200 ps (red). (d) Kinetic data in 2-MTHF (markers) and fit (full line) at 406 nm (circles, blue), 454 nm (triangles, green), and 654 nm (squares, red).

Table 2. Half-Wave Potential in DMF and Driving Force for Electron Transfer from the Singlet and Triplet State of the Porphyrin

	$E_{1/2}$ vs SCE (V)[a]			$-\Delta G^0_{ET}$ (eV)[b]	
	$ZnP^{+\bullet}$/ ZnP	ZnP/ $ZnP^{-\bullet}$	Pt(pp)/ $Pt(pp^{-\bullet})$	S_1	T_1
Pt(bpy)(eϕ)$_2$			−0.82		
Pt(tpy)(eϕ)$^+$			−0.78		
ZnTTP	0.87	−1.31			
ZnP-*m*-ϕ	0.89	−1.33			
ZnP-*β*	0.91	−1.18			
ZnP-*m*-ϕ-Pt$^+$	*c*	*c*	*c*	0.41	−0.06
(ZnP-*m*-ϕ)$_2$-Pt	0.89	*d*	−0.77	0.37	−0.10
ZnP-*β*-Pt$^+$	0.88	*d*	−0.76	0.33	−0.16
(ZnP-*β*)$_2$-Pt	*c*	*c*	*c*	0.29	−0.20
ZnP-*m*-e-Pt^{+e}	0.83	−1.20	−0.80	0.34	*f*

[a] Calculated from potential of decamethyl ferrocene vs SCE in DMF.[52] [b] ΔG^0_{ET} was estimated by the Rehm−Weller equation[61,62] (see eq A1 in the Appendix) using the redox potentials of the references **ZnP-*m*-ϕ**, **ZnP-*β***, **Pt(tpy)(eϕ)**$^+$, and **Pt(bpy)(eϕ)$_2$**. Singlet energies are calculated from the average of the 0−0 transition in absorption and fluorescence, and triplet energies are estimated from the phosphorescence peak at 77 K. [c] Not meaured due to shortage of the complexes. [d] Potential window narrowed down to avoid risk of second reduction of the platinum moiety. [e] Values taken from Monnereau et al.[41] [f] Not given.

Excitation of the porphyrin unit in dyad **ZnP-*m*-ϕ-Pt**$^+$ results in an initial spectrum that is similar to its porphyrin reference **ZnP-*m*-ϕ**, but the S_1 state rapidly decays (τ = 10 ps) to the ground state. There is however a rise (τ = 1.5 ps) and decay (τ = 10 ps) feature on the blue side of the Soret band and around the stimulated S_1 emission at 650 nm (Figure 3a,b). The cation radical of ZnP is reported to have a peak around 400 nm,[63,64] and the rise and decay behavior represents the formation and disappearance of the charge-shifted state. Note that the back reaction is faster than the forward electron transfer. Therefore, the 1.5 ps component seen as a rise of the charge-shifted intermediate is actually the recombination time, while the 10 ps component is the time constant for charge shift from the S_1 state, which matches that for the decay of the S_1 signal at, e.g., 454 nm (Figure 3b,d). This is the somewhat counterintuitive but well-known effect of the case when $k_{ET} < k_{BET}$.[65,66] The rise and decay feature at 650 nm comes from the disappearance of the stimulated emission (rise) followed by the decay of the charge shifted state. These observations indicate that the rapid quenching of the S_1 state is due to electron transfer, in agreement with the reaction scheme previously suggested by Monnereau et al.[41] for **ZnP-*m*-e-Pt**$^+$. The related triad, **(ZnP-*m*-ϕ)$_2$-Pt**, behaves very similarly, with the same spectral features and almost the same rates (τ_{ET} = 12 ps, τ_{BET} = 1.6 ps). For both compounds, there is at longer times a small feature that resembles the triplet state spectrum of **ZnP-*m*-ϕ**. The triplet features could either come from recombination to the triplet or from the fractions of unquenched porphyrin that was seen in the TCSPC measurements.

In 2-MTHF, excitation of the zinc porphyrin in **ZnP-*m*-ϕ-Pt**$^+$ results in electron transfer, but the rates for the forward and back reaction have decreased (τ_{ET} = 26 ps, τ_{BET} = 4.5 ps). The yield of the porphyrin triplet is however much higher than in DMF, which indicates that the back electron transfer partly goes to the triplet state (Figure 3c,d). This is in agreement with a lower reorganization energy in 2-MTHF, which would decrease the barrier for recombination to the triplet state (see Discussion).

β*-Linked Dyads.** The S_1 transient spectrum of **ZnP-*β has the familiar features of zinc porphyrins, but as

(61) Rehm, D.; Weller, A. *Isr. J. Chem.* **1970**, *8*, 259–271.
(62) Weller, A. *Z. Phys. Chem.* **1982**, *133*, 93–98.
(63) Okhrimenko, A. N.; Gusev, A. V.; Rodgers, M. A. J. *J. Phys. Chem. A* **2005**, *109*, 7653–7656.
(64) Petersson, J.; Eklund, M.; Davidsson, J.; Hammarström, L. *J. Am. Chem. Soc.* **2009**, *131*, 7940–7941.
(65) See any textbook on elementary consecutive kinetics of the type; A → I → C (e.g., ref 66).
(66) Engel, T.; Reid, P. *Physical Chemistry*; 1st ed.; Pearson Education: San Fransisco, CA, 2006.

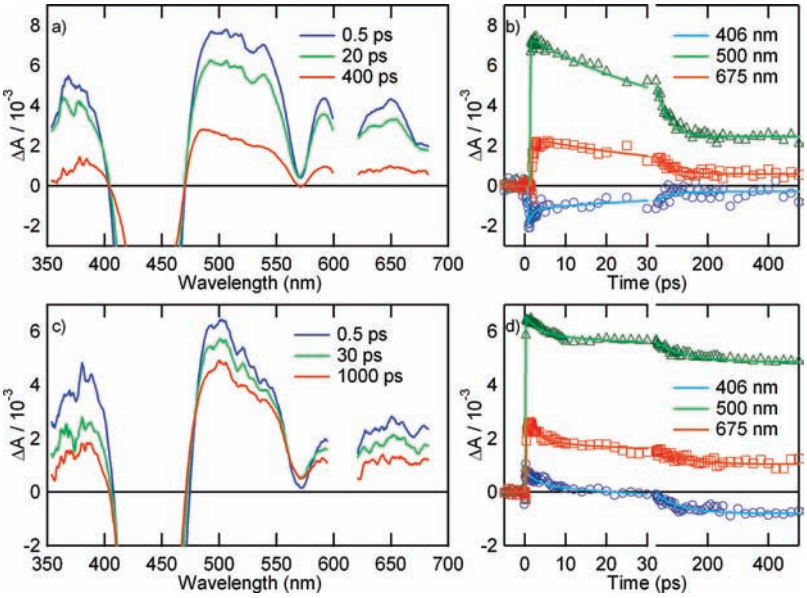

Figure 4. Results from pump−probe measurements on **ZnP-*β*-Pt**$^+$ in DMF (a and b) and in 2-MTHF (c and d), $\lambda_{exc} = 603$ nm. (a) Difference spectra in DMF at 0.5 ps (blue), 20 ps (green), and 400 ps (red). (b) Kinetic data in DMF (markers) and fit (full line) at 406 nm (circles, blue), 500 nm (triangles, green), and 675 nm (squares, red). (c) Difference spectra in 2-MTHF at 0.5 ps (blue), 30 ps (green), and 1000 ps (red). (d) Kinetic data in 2-MTHF (markers) and fit (full line) at 406 nm (circles, blue), 500 nm (triangles, green), and 675 nm (squares, red).

expected from the ground state spectrum, with a much broader Soret-band bleach and a redshift of both the bleach features and the stimulated emission signal (Figure S4b, Supporting Information). Excitation of **ZnP-*β*-Pt**$^+$ at 608 nm results in formation of the S_1 state of the zinc porphyrin. This spectrum decays with a time constant of 41 ps without any discernible rise and decay features (Figure 4a,b). Remaining after 200 ps is a spectrum of a long-lived fraction which behaves as unquenched porphyrin. In 2-MTHF, the singlet state of **ZnP-*β*-Pt**$^+$ disappears with a lower rate, and the porphyrin triplet state yield is much higher than in DMF (Figure 4c,d). The triad (**ZnP-*β***)$_2$**-Pt** in DMF shows the same transient spectral feature as **ZnP-*β*-Pt**$^+$, but with a slightly lower rate of S_1 deactivation ($\tau = 60$ ps). However, in 2-MTHF, the triad reacts faster ($\tau = 23$ ps) and almost quantitatively forms the porphyrin triplet state (Figure S5, Supporting Information).

Soret-Band Excitation. Excitation in the Soret band of the *β*-substituted porphyrins results in the spectral features of the S_1 state within the response function of the experiment, indicating that the S_2 state is too short-lived to be resolved. In contrast, the *meso*-substituted reference porphyrin **ZnP-*m*-*ϕ*** displays spectral features of the S_2 state at early times after excitation. Most notable is the stronger absorption on the blue side of the Soret band, the bleach from stimulated emission on the red side of the Soret band, and the lack of stimulated emission around 650 nm.[53,64] For **ZnP-*m*-*ϕ*** in 2-MTHF, these features disappear with a time constant of about 1.7 ps. In the *meso*-linked dyad and triad **ZnP-*m*-*ϕ*-Pt**$^+$ and (**ZnP-*m*-*ϕ***)$_2$**-Pt**, the spectral features of the S_2 state disappear with a rate constant of about 0.35 ps (Figure S6, Supporting Information). A similar quenching of the S_2 state can also be seen in DMF, but its rate is too high to be properly resolved. In both solvents, the fast deactivation still results in formation of the S_1 state, which reacts as previously described. This shows that the S_2 quenching mechanism could not be electron transfer to the lowest, relaxed charge-separated state, as this lies below the S_1 state. An interesting possibility is however that the quenching could be due to electron transfer to a higher lying charge-separated state, which undergoes ultrafast recombination to form the S_1 state. This type of mechanism has recently been observed for a zinc porphyrin−naphthalene diimide dyad.[19]

Discussion

Quenching Mechanism. Quenching of the porphyrin S_1 occurs by electron transfer as shown by the spectral features of the observed intermediate state in the *meso*-linked complexes and by the large triplet yield in the low-polarity solvent 2-MTHF. Other quenching mechanisms, such as enhanced intersystem crossing[67,68] and Dexter energy transfer, can be excluded since these mechanisms are not expected to be very solvent-dependent, and energy transfer to the lowest excited state of the Pt unit would be slightly endergonic. Table 3 summarizes the observed electron transfer rates.

The increase in triplet formation upon electron transfer recombination observed in 2-MTHF can be rationalized with Marcus theory[20,21] and the solvent dependence of ΔG^0 and reorganization energy (λ)[61,62] for photoinduced electron transfer (see eqs A1−A5 in the Appendix):

$$k_{ET} = \sqrt{\frac{\pi}{\hbar^2 \lambda k_B T}} V_{DA}^2 \exp\left(\frac{-(\Delta G^\circ + \lambda)^2}{4\lambda k_B T}\right) \qquad (1)$$

Equations A1−A5 predict that a more polar solvent will stabilize oppositely charged species formed after charge-separation and hence lower the energy of the radical ion pair. The charge-separated state for (**ZnP-*m*-*ϕ***)$_2$**-Pt** and (**ZnP-*β***)$_2$**-Pt** in 2-MTHF is shifted up in energy, and the reorganization energy is lowered, compared to the case in DMF ($\lambda \approx 0.65$ eV for **ZnP-*m*-e-Pt**$^+$).[41] This decreases the

(67) Rachford, A. A.; Goeb, S.; Castellano, F. N. *J. Am. Chem. Soc.* **2008**, *130*, 2766–2767.
(68) Danilov, E. O.; Rachford, A. A.; Goeb, S. b.; Castellano, F. N. *J. Phys. Chem. A* **2009**, *113*, 5763–5768.

Table 3. Summary of Electron Transfer Time Constants[a]

	DMF			2-MTHF	
compound	$(k_{ET})^{-1}$ (ps)	$(k_{BET})^{-1}$ (ps)	ΔG^0_{ET} (eV)	$(k_{ET})^{-1}$ (ps)	$(k_{BET})^{-1}$ (ps)
ZnP-*m*-φ-Pt$^+$	9.7 (±1.1)	1.2 (±0.1)	−0.41	24 (±4)	5.3 (±1.2)
(ZnP-*m*-φ)$_2$-Pt	13 (±1.8)	1.3 (±0.5)	−0.37	22 (*b*)	4.8 (±1.9)
ZnP-*β*-Pt$^+$	45 (±5)	*c*	−0.33	90 (±5)	*c*
(ZnP-*β*)$_2$-Pt	61 (±11)	*c*	−0.29	26 (±7)	*c*
ZnP-*m*-e-Pt^{+d}	6	*e*	−0.34	*e*	*e*

[a] Rates presented are the mean between at least two fs-TA measurements. The TCSPC data were also included for the β-linked systems. Numbers in parentheses represent one standard deviation. [b] Only one measurement was done. [c] Not detected. [d] Data from Monnereau et al.[41] [e] Not given.

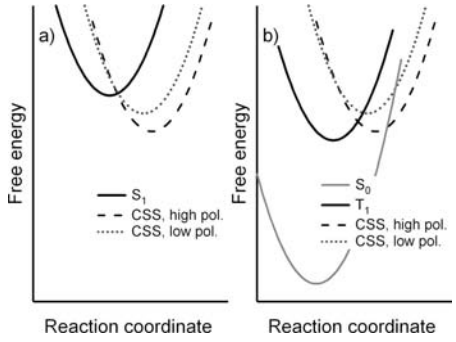

Figure 5. Generic state diagram for a charge-separation and recombination reaction, illustrating the effect of solvent polarity on the reaction barriers. (a) Electron transfer from an excited state (S_1) resulting in a charge-separated state (CSS) in high and low polarity solvents. (b) Recombination from a charge-separated state to either a low lying triplet state (T_1) or to the ground state (S_0).

reaction barrier for back electron transfer to the porphyrin triplet state (Figure 5). Concomitantly, recombination to the ground state is slowed down when going to 2-MTHF because this reaction lies in the Marcus inverted region ($-\Delta G° > \lambda$) so that its barrier instead increases. Thus, the yield of the porphyrin triplet upon recombination increases, although the net rate of recombination (the sum of triplet and singlet pathways) is somewhat lower.

For a charge shift instead of charge separation, as in dyad **ZnP-*m*-φ-Pt$^+$** and **ZnP-*β*-Pt$^+$**, the dielectric continuum model predicts that the driving force does not vary with solvent polarity, for D and A units of similar size (eqs A1−A4). The reorganization energy is still lower in low-polarity solvents (eq A5), however, which should have sufficient effect on the barriers for recombination to explain the higher triplet yield in 2-MTHF upon recombination (Figure S7, Supporting Information).

The rate of charge separation in **(ZnP-*m*-φ)$_2$-Pt** and **(ZnP-*β*)$_2$-Pt** is not expected to be strongly dependent on solvent polarity, as the variation in $\Delta G°$ and λ to a large extent gives compensatory effects on the barrier (Figure 5). The observed rate constant (k_{ET}) varies only within a factor of 2−3 between the solvents. For the charge shift from the excited porphyrin in **ZnP-*m*-φ-Pt$^+$** and **ZnP-*β*-Pt$^+$** on the other hand, one would expect a faster reaction in 2-MTHF, as λ would be lower while $\Delta G°$ would be the same as in DMF. This is not observed, however, which underscores that the continuum model predictions must be treated with some caution.[69]

(69) One of many aspects not covered in this model is the effect from the counterion. Ion pairing between the counterion and the Pt^+ unit in low-polarity solvent could make the system behave like a neutral dyad from an electrostatic point of view.

Effects on Electronic Coupling. The linking motif between the porphyrin and the OPE bridge was varied in order to lower the electronic coupling, which may lead to lower electron transfer rates. The results presented in Table 3 indicate that the electron transfer rates in DMF indeed were slowed down. A charge-transfer state could be spectroscopically detected in the *meso*-phenyl linked dyads, suggesting that this linking motif led to a stronger retardation for back reaction than the forward reaction. This partial success does not alter the fact that also all of the new ZnP−Pt dyads presented in this study show a back electron transfer that is faster than the forward reaction.

Changing the anchoring position has a large influence on the electronic coupling, and the rate is about 7 times lower when linked *via* the β position than *via* the *meso* position. This is in agreement with previous studies by Hayes et al.[46] and Song et al.,[28] who both report significantly slower electron transfer for the β isomer, see Table 4. It is well-known that S_1 and S_2 transitions have significant contributions from the two highest occupied orbitals (a_{1u} and a_{2u} symmetry).[44] The a_{1u} orbital has nodes at the *meso* position, while a_{2u} has a high electron density on the *meso* position and a lower density at the β positions (Figure 1b). Yang et al.[45] have shown that the relative reactivity for Dexter energy transfer[70] of the β and *meso* positions can be reversed by changing which of the two orbital symmetries is the HOMO. For a *meso*-phenyl substituted porphyrin (such as 5,10,15,20-tetraphenyl porphyrin), the lowest singlet state has a larger contribution from the a_{2u} orbital. This orbital has a high electron density on the *meso* position, but very little on the β position, which explains why the reactivity is higher at the *meso* position. Hayes et al. showed that this reasoning also can be applied to reactions from the S_2 state.[46] Electron transfer from the S_2 state was more rapid for the β position, in agreement with the a_{1u} orbital contributing most to this transition.

The effect on the absorption spectra and electron transfer rates of a direct ethynyl coupling of the OPE bridge to the porphyrin ring is pronounced. By coupling *via* a phenyl group instead, the steric interaction forces the phenyl and porphyrin groups out of plane, which hinders the π conjugation of the chromophore extending out on the bridge.[43] However, with an ethynyl anchoring group, the phenyl moieties of the bridge are almost free to rotate, resulting in an average dihedral angle between the chromophore and the phenyl groups that favor π conjugation.[24,71,72] The higher

(70) Dexter, D. L. *J. Chem. Phys.* **1953**, *21*, 836–850.

(71) Odobel, F.; Suresh, S.; Blart, E.; Nicolas, Y.; Quintard, J.-P.; Janvier, P.; Le Questel, J.-Y.; Illien, B.; Rondeau, D.; Richomme, P.; Haupl, T.; Wallin, S.; Hammarström, L. *Chem.—Eur. J.* **2002**, *8*, 3027–3046.

(72) Wallin, S.; Hammarström, L.; Blart, E.; Odobel, F. *Photochem. Photobiol. Sci.* **2006**, *5*, 828–834.

Table 4. Compilation of Systems Comparing Electron Transfer Activity of the *meso* and β Position of Porphyrins

reference	position	system	solvent	$(k_{ET})^{-1}$ (ps)	$(k_{BET})^{-1}$ (ps)	$k_{ET,meso}/k_{ET,\beta}$	$k_{BET,meso}/k_{BET,\beta}$
Monnereau[41]	*meso*	ZnP-eϕe-Pt$^+$	DMF	6		7.5	
this work	β	ZnP-eϕe-Pt$^+$	DMF	45			
Hayes et al.[46]	*meso*	ZnP-ϕ-PI	MTHF	17	140	7.5	5.0
	β	ZnP-ϕ-PI	MTHF	130	710		
Song et al.[28]	*meso*	H_2P-ϕeϕ-ZnP$^+$	PhCN	6	20	3.2	3.3
	β	H_2P-ϕeϕ-ZnP$^+$	PhCN	19	65		

degree of conjugation causes a perturbation of the porphyrin absorption spectra and higher electron transfer rates, as was previously shown by a direct comparison of OPE bridged Zn(II)P−Au(III)P$^+$ bis-porphyrins. Both the forward and back electron transfer were 2−3 orders of magnitude faster with coupling *via* the ethynyl group[27] than *via* the phenyl group.[73] In the present study, the difference in rate between ethynyl (**ZnP-*m*-e-Pt**$^+$) and phenyl (**ZnP-*m*-ϕ-Pt**$^+$) anchoring is less pronounced, but the latter shows a 2-fold lower forward electron transfer rate, even though the center-to-center distance is shortened from 17 to 14.5 Å. The greater difference in the previous study may possibly be the presence of β-alkyl groups on the phenyl-anchored $Zn^{(II)}P-Au^{(III)}P^+$ system[73] that force the phenyl group further out of the porphyrin plane.

Conclusion

We have synthesized a new series of zinc porphyrin−platinum polypyridyl complexes and demonstrated that they perform rapid electron transfer upon excitation of the porphyrin moiety. The back electron transfer is faster than the forward reaction, as was also found in previous ZnP−Pt dyads. Nevertheless, the charge transfer state was spectroscopically observed as an intermediate in two of the dyads, providing direct evidence for electron transfer. Also, indirect evidence for electron transfer was found from enhanced porphyrin triplet formation in the less polar 2-MTHF, attributed to charge recombination to the triplet state. Dyads linked *via* the porphyrin *meso* position showed considerably faster electron transfer rates than those linked *via* the β position. Furthermore, linking the OPE bridge to the porphyrin *via* an ethynyl instead of a phenyl group leads to much stronger electronic coupling, in agreement with some previous reports.

Appendix

For electron transfer from the excited donor, $\Delta G°$ is given by[61,62]

$$\Delta G° = e(E^{\circ}_{D^{ox}/D} - E^{\circ}_{A/A^{red}}) - E_{00} + w + C \qquad (A1)$$

For the corresponding back electron transfer ΔG^0 is given by:

$$\Delta G° = e(E^{\circ}_{A/A^{red}} - E^{\circ}_{D^{ox}/D}) - w - C \qquad (A2)$$

$E_{D^{ox}}/D°$ and $E_{A/A^{red}}°$ are the half wave potentials for the donor oxidation and acceptor reduction, and E_{00} is the excited state energy. w and C are, respectively, correction terms due to differences in Coulombic interaction between the reactants and products and for differences in redox potentials when changing the solvent. For the donor and acceptor as spheres in a dielectric continuum, one obtains

$$w = \frac{e^2}{4\pi\varepsilon_0\varepsilon}\left(\frac{(z_{D^{ox}}z_{A^{red}} - z_D z_A)}{R}\right) \qquad (A3)$$

$$C = \frac{e^2}{4\pi\varepsilon_0}\left(\frac{({z_{D^{ox}}}^2 - {z_D}^2)}{2r_D} + \frac{({z_{A^{red}}}^2 - {z_A}^2)}{2r_A}\right)\left(\frac{1}{\varepsilon} - \frac{1}{\varepsilon^{ref}}\right) \qquad (A4)$$

where e is the elementary charge, ε_0, is the permittivity in a vacuum, ε and ε^{ref} are the dielectric constants for the solvent in which the ET rate (ε) and reduction potentials (ε^{ref}) were determined, z_i is the formal charge of species i, r is the donor or acceptor radius, and R is the donor−acceptor distance. Equations A3 and A4 are often reported in the special case when the donor and acceptor reactants are neutral, i.e., $z_D = z_A = 0$.[1]

The solvent polarity dependence of the outer reorganization energy is given by[1]

$$\lambda_{out} = \frac{e^2}{4\pi\varepsilon_0}\left(\frac{1}{2r_D} + \frac{1}{2r_A} - \frac{1}{r_{DA}}\right)\left(\frac{1}{n^2} - \frac{1}{\varepsilon_{solv}}\right) \qquad (A5)$$

treating the donor and acceptor as spheres in a dielectric continuum (this is valid for D−A and D_{ox}−A_{red} pairs that are neutral or monovalent ions).

Acknowledgment. This study was partially subsidized by the Agence Nationale de la Recherche (ANR) for the project PhotoCumElec and by la Région Pays de la Loire (CPER 18007) for the salary of C.M. We also thank the Knut and Alice Wallenberg Foundation, The Swedish Energy Agency, U3MEC Uppsala, and COST D35 for financial support.

Supporting Information Available: Key to labels in ^{1}H NMR data, reported in the experimental section; synthesis and characterization of compound 3, 4, 7, 8, 11 and 15; comparison between absorption spectra of donor−acceptor dyads and references; absorption and emission properties in 2-MTHF; emission spectra in DMF; additional fs-TA pump probe data; reactions from the porphyrin S2-state; and state diagram for electron transfer reaction in charge−shift compounds. This material is available free of charge via the Internet at http://pubs.acs.org.

(73) Wiberg, J.; Guo, L.; Pettersson, K.; Nilsson, D.; Ljungdahl, T.; Martensson, J.; Albinsson, B. *J. Am. Chem. Soc.* **2007**, *129*, 155–163.